

# Implications of doping and depletion on the switching characteristics in polymer-based organic field-effect transistors

著者	Tiwari Shashi, Pandey Manish, Takashima Wataru, Nagamatsu Shuichi, Balasubramanian S.K., Hayase Shuzi, Pandey Shyam S., Prakash Rajiv
journal or publication title	Organic Electronics
volume	56
page range	152-158
year	2018-02-12
URL	<a href="http://hdl.handle.net/10228/00007611">http://hdl.handle.net/10228/00007611</a>

doi: info:doi/10.1016/j.orgel.2018.02.012

# Implications of Doping and Depletion on the Switching Characteristics in Polymer-based Organic Field-effect Transistors

Shashi Tiwari<sup>a</sup>, Manish Pandey<sup>b</sup>, Wataru Takashima<sup>b</sup>, Shuichi Nagamatsu<sup>c</sup>,  
S. K. Balasubramanian<sup>a</sup>, Shuzi Hayase<sup>b</sup>, Shyam S. Pandey<sup>b\*</sup> and Rajiv Prakash<sup>d\*</sup>

<sup>a</sup>*Department of Electronics Engineering, Indian Institute of Technology (Banaras Hindu University),  
Varanasi-221005, INDIA.*

<sup>b</sup>*Graduate School of Life Science and Systems Engineering, Kyushu Institute of Technology,  
2-4 Hibikino, Wakamatsu, Kitakyushu 808-0196, JAPAN.*

<sup>c</sup>*Department of Computer Science and Systems Engineering, Kyushu Institute of Technology,  
680-4 Kawazu, Iizuka, Fukuoka 820-8502, JAPAN.*

<sup>d</sup>*School of Materials Science and Technology, Indian Institute of Technology (Banaras Hindu University),  
Varanasi-221005, INDIA.*

## Abstract

An effective approach for tuning the electronic characteristics of polymer-based organic field-effect transistors (OFETs) consisted of Poly(3-hexylthiophene) (P3HT) doped with 7,7,8,8-tetracyanoquinodimethane (TCNQ) and depletion layer formed by Al-coating is being reported. Doping of P3HT was employed to accumulate and tune the carrier concentration while implementation of depletion layer leads to reduce the channel conductance. It has been demonstrated that on-currents in the OFETs were enhanced with the extent of TCNQ doping from 0% to 20% in the P3HT. Upon introduction of a thin layer of Al led to the formation of a depletion region resulting in to further decrease in the off-state current along with the improvement in the subthreshold characteristics. These two procedures, thus, provide counter-

effects in terms of the on-state characteristics by doping and the off-state characteristics by depletion, which promotes switching performance in OFETs indicating the potentiality of doping technology for organic electronics.

**Keywords:** Field-effect transistor; TCNQ doping; Depletion layer; P3HT; Aluminum

## 1. Introduction

Solution processable organic semiconductors have attracted huge attentions owing to the facile thin film fabrication of active semiconductor layer in organic electronic devices. Organic semiconductors based on  $\pi$ -conjugated polymers needs subtle control of their thin film morphology and plays a dominant role in controlling the charge transport properties [1–3]. Recent past has witnessed the report of versatile procedures for the fabrication of thin films of organic semiconductor layer in order to improve the performance of organic electronic devices aiming towards their practical application [4–6]. Organic field-effect transistors (OFETs) are the one of the most investigated devices aiming toward practical realization of the cost-effective flexible circuits and high throughput large area device fabrication. OFET essentially operates as the electronic switch by changing the channel conductance form insulative to conductive. In a typical OFET device configuration, thin semiconductor layer is coated on to a planar-type conductor (source and drain), thus the device performance is highly sensitive to the nature of this semiconducting film on the gate insulator. Efforts are now being directed towards enhancement in both of the charge carrier mobility and environmental stability not only by design and development novel organic semiconductors but also the device structure in order to achieve the practical realization of high-performance OFETs [7]. Implementation and control of the highly-

doped as well as depletion region in electronic devices has been identified as one of the important technologies for the fast growing Si-based electronics. High-performance electronic circuits fabricated by sophisticated and controlled doping are already in the practical use but simplification of such processing is expected to broaden to the applications potentials. Specific control on the population of both of the electrons and holes is crucial to design the conductive/insulative-regions is one of the key-parameters for building the electronic circuits. Moreover, doping of organic semiconductors by donor/accepter moieties has also been effectively employed in order to control and achieve the balanced carrier concentrations [8,9].

Simultaneous control of carrier density of both of the electrons and holes in single material especially in the organic semiconductors is cumbersome and, therefore, control of the single carrier has been widely investigated. Molecular doping assisted by oxidation and reduction of organic semiconductors has been considered to be convenient way to tune their electronic properties for a targeted applications in order to introduce desired extent of equilibrium charge carriers [10,11]. In this context, conjugated polymers (CPs) are capable to form thin-films with uniform doping simply by mixing them with acceptors via solution process. Relative solubility issues of CPs and acceptor molecules sometimes hinders molecular level mixing and homogeneous in the blend films and poses difficulty for attaining the tunable and reproducible carrier concentrations. To circumvent this issue, Scholes et al reported an interesting sequential processing technique for fabricating high quality homogeneous films of regioregular poly(3-hexylthiophene) (RR-P3HT) doped with acceptor molecules providing doped polymeric films with tunable and reproducible electrical conductivities [12]. Effective utilization of such doping induced carrier control in CPs is very important for the development new class

functional organic materials with improved device functionality. In contrast to the carrier accumulation by doping in organic semiconductors, chemical strategies such as reduction of CPs under basic conditions like ammonia gas have also been successfully utilized to suppress the concentration of holes [13–15]. These methods, however, are difficult to employ directly for designing the nano-scale carrier distribution particularly for organic transistors. P3HT has been widely used as typical p-type semi-conducting material for a number of organic electronic devices [16–18]. Introduction of acceptor moieties in P3HT led to enhancement of the film conductance by doping. Besides this, P3HT is well known to show diode characteristics with Au and Al being used as anode and cathode electrodes, respectively. Mechanism of the rectification observed in such diodes is attributed to the formation of depletion layer at Al/P3HT interface owing to the formation of Schottky contact. We have also demonstrated that there was a decrease in the conductance of P3HT thin-film with over-coating a thin (about 10 nm) Al, which is due to the formation of depletion layer in P3HT thin-films [19]. These characteristics indicate that a thin-Al-coating is possible key-method to decrease the film conductance like dedoping process for conjugated polymers.

Herein, we would like to propose a novel strategy to control the channel conductance of polymer-based OFET, by acceptor assisted doping of P3HT, which was used as active layer of OFET by solution process [17]. Doping of P3HT with 7,7,8,8 tetracyanoquinodimethane (TCNQ) was employed to accumulate the carriers along with the implementation of depletion layer by coating of a thin layer of Al to reduce the channel conductance. Finally, it has also been demonstrated that carrier accumulation with TCNQ improved the on-state channel-conductance

and the depletion of carriers with Al-coating promoted both the off-state and the on-set characteristics.

## 2. Experimental details

Highly p-doped silicon with thermally grown thin-film (300 nm) of SiO<sub>2</sub> ( $C_{ox} = 10$  nF/cm<sup>2</sup>) layer was used as gate dielectrics as well as gate electrode for OFETs. First of all, SiO<sub>2</sub> surface was made hydrophilic by surface treatment with solution of aqueous ammonia, distilled water and hydrogen peroxide (1:2:1) for 1.5 h at 100 °C. Purpose of this hydrophilic surface treatment was to create active –OH functionality on surface, which assists the formation of self-assembled layer. Considering the hydrophobic nature of P3HT, SiO<sub>2</sub> surface was made hydrophobic by placing the substrates in a 10 mM octyltrichlorosilane (OTS) in dehydrated toluene. After OTS treatment, substrates were again washed thoroughly with dehydrated-toluene followed by heating at 150°C for 10 min. Transparent glass slides were also treated in the same way in order to make samples for other characterizations.

Chemical structure of P3HT and TCNQ is shown in **Fig. 1**. TCNQ was purchased from Tokyo Kasei and used as received. Regioregular poly-3-hexylthiophene (P3HT) was synthesized and purified as per reported in the literature [20]. Various concentrations of the TCNQ/P3HT solution (1%, 5%, 10% and 20% of TCNQ/thiophene unit of P3HT) were prepared by mixing 0.2 weight % P3HT/toluene and 0.1 weight % TCNQ/acetone solutions. Each of the TCNQ doped P3HT solutions were heated before spin coating at a speed of 3000 rpm (~21 nm) and 1500 rpm (~ 32 nm) for 1 min. For fabricating OFET, gold was utilized as source and drain electrodes and 40 nm of gold was deposited on semiconductor layer through Ni-shadow mask having the

channel length ( $L$ ) and width ( $W$ ) of 20  $\mu\text{m}$  and 2 mm, respectively by thermal vapor deposition at base pressure of  $2 \times 10^{-6}$  Torr. Electronic characteristics were measured in vacuum at about  $10^{-6}$  Torr with computer controlled KEITHLEY 2612 two-channel electrometer. The average thickness of P3HT film was measured with surface profiler (DEKTAK 6M) or estimated by the peak intensity of absorption spectra by V-570 spectrophotometer with the absorption coefficient of P3HT as about  $6.5 \times 10^4/\text{cm}$  [21]. Surface morphologies were observed by atomic force microscope (AFM) with JEOL SPM5200 and Olympus probe (OMCL-AC200TS-C3).

## Results and Discussion

Surface morphologies of P3HT films are shown in **Fig. 2**. A relatively flat surface was observed in a pristine P3HT film while all of the TCNQ doped P3HT films exhibited fine particles and/or fibrous structures. Particularly, nano-fiber like structures were clearly visible in doped samples which get more pronounced with increasing the extent of TCNQ. Formation of nanofibrous structures could be attributed to the relatively poor solubility of the P3HT in toluene as compared to the commonly used chloroform. It has also been reported that P3HT tends to form nano-fibers in a relatively poor solvents or addition of trace amounts of non-solvents of P3HT [18,22]. The film casting from the mixture of P3HT/toluene with TCNQ/acetone promotes the nano-structure formations possibly due to their hampered solubility in corresponding solvents used for present investigation. It should be noted that the surface morphology of Al-coated one (Fig. 2f) shows interesting surface morphology where, well-grown particles having diameter of 150-200 nm covers the entire surface. Although the mechanism to form the particles is not well-understood and the particle size is larger than the thickness of the

Al deposition (50 nm), this image evidences to cover the surface with some Al particles after the thermal evaporation.

Figure 3(a) shows the output characteristics of OFETs fabricated using pristine and doped P3HT films. A perusal of this figure indicates a clear non-linear source-drain current ( $I_{DS}$ )-threshold voltage ( $V_{DS}$ ) characteristics even for the OFETs fabricated using P3HT doped with TCNQ. This indicates that the doped-P3HT too is able to modulate the channel conductance via field-effect. The pinch-off characteristics become unclear as a function of the doping ratio. This also corresponds to the positive shift of the  $V_{TH}$  as seen in the transfer characteristics Fig. 3(b). The magnitudes of  $I_{DS}$  were found to increase as function of doping of P3HT with TCNQ. This indicates that TCNQ having a relatively shallow energy level of lowest unoccupied molecular orbital (around 4.2 eV) still work as acceptor site for accumulating holes in P3HT. However, doping strength of TCNQ is weaker as compared to that its fluorine substituted derivative F4TCNQ, to modulate the channel conductance, transfer characteristics are quite similar to those obtained with F4TCNQ [23].

Cyclic output characteristics ( $I_{DS}$ - $V_{DS}$ ) as well as transfer characteristics ( $I_{DS}^{1/2}$ - $V_{GS}$ ) for all of the OFETs operated at  $V_{GS} = -60$  V are shown in **Fig. 3**. Various electronic parameters such as field-effect mobility in the saturation ( $\mu_{sat}$ ) as well as in linear region ( $\mu_{lin}$ ), and trans-conductance ( $g_m$ ) for all the devices were calculated using equations (1) (2) and (3), respectively [24,25].

$$I_{DSsat} = \frac{WC_{OX}\mu_{sat}}{2L}(V_{GS} - V_{TH})^2 \quad (1)$$

$$I_{DSlin} = \frac{W}{L}C_{OX}\mu_{lin}[(V_{GS} - V_{TH})V_{DS}] \text{ where } |V_{DS}| \ll |V_{GS} - V_{TH}| \quad (2)$$

$$g_m = \frac{W\mu_{sat}C_{OX}}{L}(V_{GS} - V_{TH}) \quad (3)$$

Where,  $W$  and  $L$  are the channel width and length, respectively.  $I_{DS,sat}$  is the saturated output current,  $V_{TH}$  is the threshold voltage, and  $C_{ox}$  is the gate insulating layer ( $\text{SiO}_2$ ) capacitance per unit area. In addition, an upper limit of charge trap density,  $N$ , at the interface between semiconductor and insulator was estimated with the sub-threshold swing of  $S$  as given in equation (4):

$$N = \left[ \frac{qS \cdot \log(e)}{k_B T} - 1 \right] \frac{C_{OX}}{q} \quad (4)$$

where,  $q$ ,  $e$ ,  $k_B$  and  $T$  are the elemental charge, natural logarithm, Boltzmann constant, and temperature, respectively.

Various electronic parameters for OFETs estimated with varying active channel components has been shown in the Fig. 4 along with summarization of extracted results in the table 1. It can be seen from the perusal of Fig. 4 and Table 1, that  $\mu_{sat}$ ,  $\mu_{lin}$  and  $g_m$  are increases with the increasing dopant (TCNQ) concentration indicating the contribution of doping for controlling the performance for FET in the on state. In majority of organic polymeric semiconductors, the low charge carrier mobility is the main issue for their poor device semiconductor performance. Existence of the resistance between electrode and organic semiconductor (contact resistance) or the resistance between organic semiconductor domains

(domain-boundary) has been reported to hinder the charge carrier transport [26,27]. It should be noted that the AFM images shown in the **Fig. 2** show the fibrous morphology on the doped surface. Such fibrous structure possibly connects the neighboring domains effectively. It is also reported that the nanofiber structure promotes the carrier transport for P3HT [28,29]. These findings indicate that the TCNQ doping probably contributes to increase the carrier transport by reducing the contact resistance and/or inter-domain resistances due to the formation nano-fibrous structures [3,28].

A perusal of the electronic characteristics shown in the in **Fig. 4** are very similar to those reported for OFETs based on P3HT doped with F4-TCNQ as reported by Ma et al but only difference is that we have used much higher extent of TCNQ as a dopant in this work [17]. This large difference about use of higher amount of dopant in our work is associated with the differences in the electro affinity, where doping strength of TCNQ is weaker than F4-TCNQ [23]. Therefore, relatively large-amount of TCNQ is required to dope P3HT-channel heavily as compared to F4-TCNQ. Moreover, the low electron affinity of TCNQ also enable us to vary the doping ratio in wide window to tune the OFET characteristics more precisely. Increase in the extent of doping leads to increase in the domain conductance, which concomitantly improves the  $I_{DS}$  in on-state. On the other hand,  $V_{TH}$  shifts towards positive  $V_{GS}$  and the off-state current,  $I_{OFF}$ , stays high (Fig. 3 (c)). The dynamic range of  $I_{DS}$ , therefore, reduces and suppression in the switching performance of FET results in low on/off ratio as shown in Fig. 3 (c) and Fig. 4 (c).

Step increase of  $I_{DS}$  from off-state indicates a clear switching behavior which suggested us analyze the subthreshold characteristics also known as subthreshold swing ( $S$ ) which is one of

the important parameters to characterize the switching performance of the OFETs.  $S$  was extracted by putting a linear fit to the  $\log(I_{DS})$  from onset of the  $I_{DS}$  [30]. It can be clearly seen from the eqn. (4) that  $S$  is also related to the surface trap density ( $N$ ). Variation of  $V_{TH}$  and  $S$  with the varying TCNQ concentration in P3HT is shown in **Fig. 4** indicates that increasing extent of TCNQ leads to the positive shift of  $V_{TH}$  and the increase of  $S$  (and  $N$ ) coincidentally as shown in the in Fig.3(c). Interestingly, Yamagishi et al have also made similar observation about enhancement in the  $V_{TH}$  and  $S$  upon the extent of molecular doping in OFETs [31]. Incorporation of dopant molecules in polymeric matrix may form a nanoscale mixture of both the doped and undoped regions which might lead complicated electron injection This could be responsible for increase in the  $S$  and  $N$  by TCNQ doping.

It well known that there is formation Schottky contact the interface with P3HT with metals like Al, Mg having shallow fermi energy level ( $E_F$ ) [19]. The formation Schottky junction at Al/P3HT interface is caused by the electron-donation from Al to P3HT followed by depleting holes in P3HT. Apart from demonstration of Schottky junction at Al/P3HT interface, a depletion layer width of about 17 nm has been reported by the Singh et al using photoluminescence (PL) quenching technique in Al/P3HT/ITO diodes [32]. In this work, effort was also directed to probe the implication of Schottky barrier formed by thermal evaporation of Al after spin-coating of active semi-conductor layer (21 nm) over the highly-doped P3HT channel of OFET. It can be seen that after the Al-coating,  $V_{TH}$  was reduced to 15 V (Fig. 4 (b)) along with the observation of a clear off-state in the transfer characteristics. At the same time, on-set characteristics became sharp along with the reduction in both of the  $S$  and  $N$  (Fig. 4 (d)). The output-characteristics of highly doped OFETs also exhibited relatively clear pinch-off characteristics after Al-coating (Fig.

3 (b). These results indicate that electron-donation from Al reduces channel conductance by depleting the highly-doped P3HT layer which has been schematically illustrated in the Fig. 5. Considering the thickness of active semiconductor layer over the channel (21 nm) and width of depletion layer (17 nm) as reported by Singh et al, indicates that active doped-P3HT used over the channel is almost depleted. Therefore, it can be concluded that coating thin Al to form Schottky barrier at Al/P3HT interface contributes to promote the off-state and the on-set characteristics for highly-doped OFETs.

It can be seen from Fig. 3(c) that OFETs based on doped P3HT with relatively thicker active semiconducting layer (about 32 nm) exhibits higher on-state current which is attributed to relatively thicker conducting channel since depletion width will remain unchanged. Therefore, the P3HT thickness is also important for the doped-OFET performance. It has also been reported depletion layer width in Al/P3HT Schottky devices also varies with applied external bias as confirmed by bias dependent PL quenching [33]. In this present work, OFET channels are being modulated by the Schottky contacts, therefore, formation of depletion layer of doped P3HT in MIS capacitor is also expected partially biased by the  $V_{GS}$ . Therefore, applied  $V_{GS}$  will also be involved in the modulation of the remaining conducting region of highly-doped P3HT. This explanation is also supported by the results exhibited by Fig. 3(c), where there was a sudden increase in the off-current, when thickness of P3HT layer was increased from 21 nm to 32-nm-thick, resulting in to the decreased on/off ratio. This indicates that the thickness ratio of depletion and remaining conduction region controls the off-state characteristics of the OFETs. A subtle tuning and optimization of the doping ratio, thickness of P3HT layer and the top Al coating are

expected to provide optimum performance of by implementing the doping/depleting technology for organic thin-film transistors.

## **Conclusions**

In summary, we have fabricated TCNQ doped P3HT-FETs and studied the effect of doping concentrations on the OFET performance. AFM investigations revealed morphology of thin films was found to be affected by TCNQ doping leading to nanofibrous surface. A wide range of TCNQ concentrations from 0 to 20% were conducted in order to investigate the effect of acceptor doping on the OFET characteristics. It was observed that the field-effect mobility was increased monotonically as a function of extent of doping of P3HT by TCNQ. On/off ratio was improved at low doping concentrations from 0 to 5 % and then suppressed for further increase of the dopant concentrations. To circumvent this, thin Al was thermally deposited to form Schottky contact with P3HT leading to formation of depletion layer in the doped-channel. In the light of contributions from both of the doping and the depletion in the fabricated OFETs, it has been shown that doping improves the on-state performance while depletion promotes the on-set and the off-state characteristics. Although these two characteristics play a sort of counterpart to each other, by turning the doping ratio and the thickness, the OFET characteristics can modulated for getting the optimized performance by the doping/depleting technology.

## References

- [1] J.F. Chang, B. Sun, D.W. Breiby, M.M. Nielsen, T.I. Sölling, M. Giles, I. McCulloch, H. Sirringhaus, Enhanced Mobility of poly(3-hexylthiophene) transistors by spin-coating from high-boiling-point solvents, *Chem. Mater.* 16 (2004) 4772–4776.  
doi:10.1021/cm049617w.
- [2] M. Pandey, S. Nagamatsu, W. Takashima, S.S. Pandey, S. Hayase, Interplay of Orientation and Blending: Synergistic Enhancement of Field Effect Mobility in Thiophene-Based Conjugated Polymers, *J. Phys. Chem. C.* 121 (2017) 11184–11193.  
doi:10.1021/acs.jpcc.7b03416.
- [3] M. Pandey, S. Nagamatsu, S.S. Pandey, S. Hayase, W. Takashima, Enhancement of carrier mobility along with anisotropic transport in non-regiocontrolled poly ( 3-hexylthiophene ) films processed by floating film transfer method, *Org. Electron.* 38 (2016) 115–120. doi:10.1016/j.orgel.2016.08.003.
- [4] H.R. Tseng, H. Phan, C. Luo, M. Wang, L.A. Perez, S.N. Patel, L. Ying, E.J. Kramer, T.Q. Nguyen, G.C. Bazan, A.J. Heeger, High-mobility field-effect transistors fabricated with macroscopic aligned semiconducting polymers, *Adv. Mater.* 26 (2014) 2993–2998.  
doi:10.1002/adma.201305084.
- [5] M. Pandey, S.S. Pandey, S. Nagamatsu, S. Hayase, W. Takashima, Solvent driven performance in thin floating-films of PBTTT for organic field effect transistor: Role of macroscopic orientation, *Org. Electron.* 43 (2017) 240–246.  
doi:10.1016/j.orgel.2017.01.031.
- [6] J. Soeda, H. Matsui, T. Okamoto, I. Osaka, K. Takimiya, J. Takeya, Highly Oriented Polymer Semiconductor Films Compressed at the Surface of Ionic Liquids for High-

- Performance Polymeric Organic Field-Effect Transistors, *Adv. Mater.* 26 (2014) 6430–6435. doi:10.1002/adma.201401495.
- [7] I. McCulloch, M. Heaney, M.L. Chabinyc, D. DeLongchamp, R.J. Kline, M. C?lle, W. Duffy, D. Fischer, D. Gundlach, B. Hamadani, R. Hamilton, L. Richter, A. Salleo, M. Shkunov, D. Sparrowe, S. Tierney, W. Zhang, Semiconducting thienothiophene copolymers: Design, synthesis, morphology, and performance in thin-film Organic transistors, *Adv. Mater.* 21 (2009) 1091–1109. doi:10.1002/adma.200801650.
- [8] Y. Liao, X. Liu, Enhanced Performance of Organic Light Emitting Device by Dual Doping of LiF in ETL and HTL, *J. Electrochem. Soc.* 157 (2010) H759–H762. doi:10.1149/1.3428372.
- [9] M. Pfeiffer, T. Fritz, J. Blochwitz, A. Nollau, B. Plönnigs, A. Beyer, K. Leo, Controlled Doping of Molecular Organic Layers: Physics and Device Prospects, *Adv. Solid State Phys.* 39 (1999) 77–90. doi:10.1007/BFb0107466.
- [10] C.P. Jarrett, R.H. Friend, A.R. Brown, D.M. De Leeuw, Field effect measurements in doped conjugated polymer films: Assessment of charge carrier mobilities, *J. Appl. Phys.* 77 (1995) 6289–6294. doi:10.1063/1.359096.
- [11] Y.H. Kim, S. Hotta, A.J. Heeger, Photoexcitation and doping studies of poly(3-methylthienylene), *Phys. Rev. B.* 38 (1988) 5490–5495. doi:10.1103/PhysRevB.36.7486.
- [12] D.T. Scholes, S.A. Hawks, P.Y. Yee, H. Wu, J.R. Lindemuth, S.H. Tolbert, B.J. Schwartz, Overcoming Film Quality Issues for Conjugated Polymers Doped with F4TCNQ by Solution Sequential Processing: Hall Effect, Structural, and Optical Measurements, *J. Phys. Chem. Lett.* 6 (2015) 4786–4793. doi:10.1021/acs.jpcclett.5b02332.
- [13] T. Someya, H.E. Katz, A. Gelperin, A.J. Lovinger, A. Dodabalapur, Vapor sensing with

- $\alpha,\omega$ -dihexylquarterthiophene field-effect transistors: The role of grain boundaries, *Appl. Phys. Lett.* 81 (2002) 3079–3081. doi:10.1063/1.1514826.
- [14] S. Tiwari, A.K. Singh, L. Joshi, P. Chakrabarti, W. Takashima, K. Kaneto, R. Prakash, Poly-3-hexylthiophene based organic field-effect transistor: Detection of low concentration of ammonia, *Sensors Actuators B Chem.* 171–172 (2012) 962–968. doi:10.1016/j.snb.2012.06.010.
- [15] P.K. Sahu, M. Pandey, C. Kumar, S.S. Pandey, W. Takashima, V.N. Mishra, R. Prakash, Air-stable vapor phase sensing of ammonia in sub-threshold regime of poly(2,5-bis(3-tetradecylthiophen-2yl)thieno(3,2-b)thiophene) based polymer thin-film transistor, *Sensors Actuators, B Chem.* 246 (2017) 243–251. doi:10.1016/j.snb.2017.02.063.
- [16] S. Tiwari, W. Takashima, S. Nagamatsu, S.K. Balasubramanian, R. Prakash, A comparative study of spin coated and floating film transfer method coated poly (3-hexylthiophene)/poly (3-hexylthiophene)-nanofibers based field effect transistors, *J. Appl. Phys.* 116 (2014) 94306. doi:10.1063/1.4894458.
- [17] L. Ma, W.H. Lee, Y.D. Park, J.S. Kim, H.S. Lee, K. Cho, High performance polythiophene thin-film transistors doped with very small amounts of an electron acceptor, *Appl. Phys. Lett.* 92 (2008) 63310. doi:10.1063/1.2883927.
- [18] W.D. Oosterbaan, V. Vrindts, S. Berson, S. Guillerez, O. Douhéret, B. Ruttens, J. D’Haen, P. Adriaensens, J. Manca, L. Lutsen, D. Vanderzande, Efficient formation, isolation and characterization of poly(3-alkylthiophene) nanofibres: probing order as a function of side-chain length, *J. Mater. Chem.* 19 (2009) 5424. doi:10.1039/b900670b.
- [19] K. Rikitake, D. Tanimura, W. Takashima, K. Kaneto, Investigation of depletion layer at interface of poly(3-hexylthiophene) and aluminum, *Japanese J. Appl. Physics, Part 1*

- Regul. Pap. Short Notes Rev. Pap. 42 (2003) 5561–5562. doi:10.1143/JJAP.42.5561.
- [20] S. Tiwari, W. Takashima, S.K. Balasubramanian, S. Miyajima, S. Nagamatsu, S.S. Pandey, R. Prakash, P3HT-fiber-based field-effect transistor: Effects of nanostructure and annealing temperature, *Jpn. J. Appl. Phys.* 53 (2014) 21601. doi:10.7567/JJAP.53.021601.
- [21] W. Takashima, S.S. Pandey, T. Endo, M. Rikukawa, K. Kaneto, Effects of regioregularity on carrier transport in poly(alkylthiophene) films with various alkyl chain lengths, *Curr. Appl. Phys.* 1 (2001) 90–97. doi:10.1016/S1567-1739(00)00018-3.
- [22] S. Samitsu, T. Shimomura, S. Heike, T. Hashizume, K. Ito, Field-effect carrier transport in poly(3-alkylthiophene) nanofiber networks and isolated nanofibers, *Macromolecules*. 43 (2010) 7891–7894. doi:10.1021/ma101655s.
- [23] Y. Takahashi, T. Hasegawa, Y. Abe, Y. Tokura, G. Saito, Organic metal electrodes for controlled p- and n-type carrier injections in organic field-effect transistors, *Appl. Phys. Lett.* 88 (2006) 73504. doi:10.1063/1.2173226.
- [24] B.G. Streetman, S.K. Banerjee, *Solid state electronic devices*, Pearson Prentice Hall, 2005.
- [25] S.M. Sze, K.K. Ng, *Physics of Semiconductor Devices*, 2007. doi:10.1049/ep.1970.0039.
- [26] L. Schulz, E.-J. Yun, A. Dodabalapur, Effects of contact resistance on the evaluation of charge carrier mobilities and transport parameters in amorphous zinc tin oxide thin-film transistors, *Appl. Phys. A*. 115 (2014) 1103–1107. doi:10.1007/s00339-014-8422-3.
- [27] J. Rivnay, L.H. Jimison, J.E. Northrup, M.F. Toney, R. Noriega, S. Lu, T.J. Marks, A. Facchetti, A. Salleo, Large modulation of carrier transport by grain-boundary molecular packing and microstructure in organic thin films, *Nat. Mater.* 8 (2009) 952–958. doi:10.1038/nmat2570.
- [28] M. Chang, J. Lee, N. Kleinhenz, B. Fu, E. Reichmanis, Photoinduced anisotropic

- supramolecular assembly and enhanced charge transport of poly(3-hexylthiophene) thin films, *Adv. Funct. Mater.* 24 (2014) 4457–4465. doi:10.1002/adfm.201400523.
- [29] R.J. Kline, M.D. McGehee, E.N. Kadnikova, J. Liu, J.M.J. Fréchet, M.F. Toney, Dependence of regioregular poly(3-hexylthiophene) film morphology and field-effect mobility on molecular weight, *Macromolecules*. 38 (2005) 3312–3319. doi:10.1021/ma047415f.
- [30] M. McDowell, I.G. Hill, J.E. McDermott, S.L. Bernasek, J. Schwartz, Improved organic thin-film transistor performance using novel self-assembled monolayers, *Appl. Phys. Lett.* 88 (2006). doi:10.1063/1.2173711.
- [31] Y. Yamagishi, K. Noda, H. Yamada, K. Matsushige, Organic field-effect transistors with molecularly doped polymer gate buffer layer, *Synth. Met.* 162 (2012) 1887–1893. doi:10.1016/j.synthmet.2012.08.020.
- [32] V. Singh, A.K. Thakur, S.S. Pandey, W. Takashima, K. Kaneto, Characterization of depletion layer using photoluminescence technique, *Appl. Phys. Express*. 1 (2008) 21801. doi:10.1143/APEX.1.021801.
- [33] V. Singh, A.K. Thakur, S.S. Pandey, W. Takashima, K. Kaneto, Evidence of photoluminescence quenching in poly(3-hexylthiophene-2,5-diyl) due to injected charge carriers, *Synth. Met.* 158 (2008) 283–286. doi:10.1016/j.synthmet.2008.01.013.

## Figure captions

**Figure 1.** Chemical structure of P3HT (a) and TCNQ (b).

**Figure 2.** AFM images of P3HT films: (a) pristine, (b) 1% TCNQ, (c) 5% TCNQ, (d) 10% TCNQ, (e) 20% TCNQ and (f) 20% TCNQ with thin-Al coating. The scale bar represents 1  $\mu\text{m}$  (250 nm in the insets).

**Fig. 3.** Schematic structure of OFET and electronic characteristics. Output characteristics at  $V_{GS} = -60$  V (a), transfer characteristics at  $V_{DS} = -60$  V (b) and semi-logarithmic replots of transfer characteristics in (c).

**Figure 4.** Variation of different electronic parameters in OFET as a function of different channel configurations. (a) Mobility, (b) Threshold voltage and transconductance, (c) On/Off ratio, (d) Subthreshold swing and charge trap density.

**Figure 5.** Schematic drawing of the off- (upper) and on-states (lower panel) of P3HT OFETs with and without doped (and depleted) region. The deeper orange color represents the higher conductance.

**Table 1.** Electronic parameters of the OFETs as a function of different configuration of channel.

<b>FET channel</b>	$V_{TH}$ (V)	$\mu_{sat}$ ( $\text{cm}^2/\text{Vs}$ )	$\mu_{lin}$ ( $\text{cm}^2/\text{Vs}$ )	$i_{on}$ (A)	$i_{off}$ (A)	<b>on/off ratio</b>	$S$ (V/dec)	$N$ ( $\times 10^{12}/\text{cm}^2$ )	$g_m$ (nS)
pristine	5	$9.6 \times 10^{-5}$	$5.4 \times 10^{-5}$	$1.2 \times 10^{-6}$	$1.4 \times 10^{-9}$	$10^{2.9}$	5	2.3	6.2
1 % doped	14	$8.1 \times 10^{-4}$	$6.4 \times 10^{-4}$	$3.1 \times 10^{-6}$	$9.9 \times 10^{-10}$	$10^{3.5}$	10	4.7	60
5%	16	$2.5 \times 10^{-3}$	$1.8 \times 10^{-3}$	$7.3 \times 10^{-6}$	$8.2 \times 10^{-10}$	$10^{3.9}$	14	6.6	190
10 %	30	$3.1 \times 10^{-3}$	$2.3 \times 10^{-3}$	$1.6 \times 10^{-5}$	$4.9 \times 10^{-9}$	$10^{3.5}$	17	8.1	280
20 %	65	$5.4 \times 10^{-3}$	$5.3 \times 10^{-3}$	$6.4 \times 10^{-5}$	$6.2 \times 10^{-6}$	$10^{1.0}$	95	45.4	670
20 % Al (21 nm PHT)	15	$3.6 \times 10^{-3}$	$2.2 \times 10^{-3}$	$1.6 \times 10^{-5}$	$1.5 \times 10^{-9}$	$10^{4.0}$	10	4.7	200
20 % Al (32 nm PHT)	10	$1.9 \times 10^{-2}$	$9.6 \times 10^{-3}$	$2.4 \times 10^{-5}$	$1.2 \times 10^{-8}$	$10^{3.3}$	18	8.0	1300

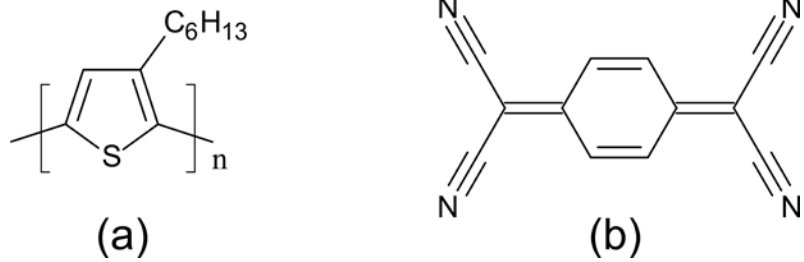


Figure 1

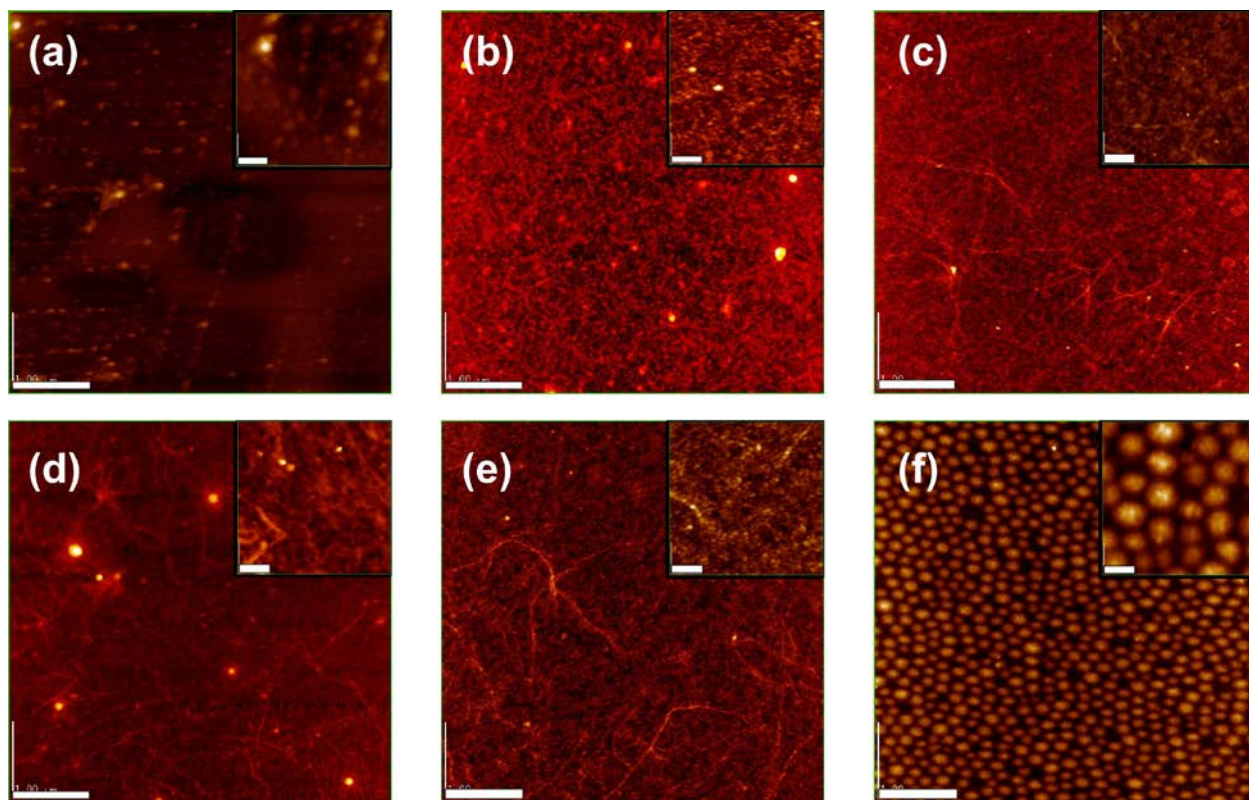


Figure 2

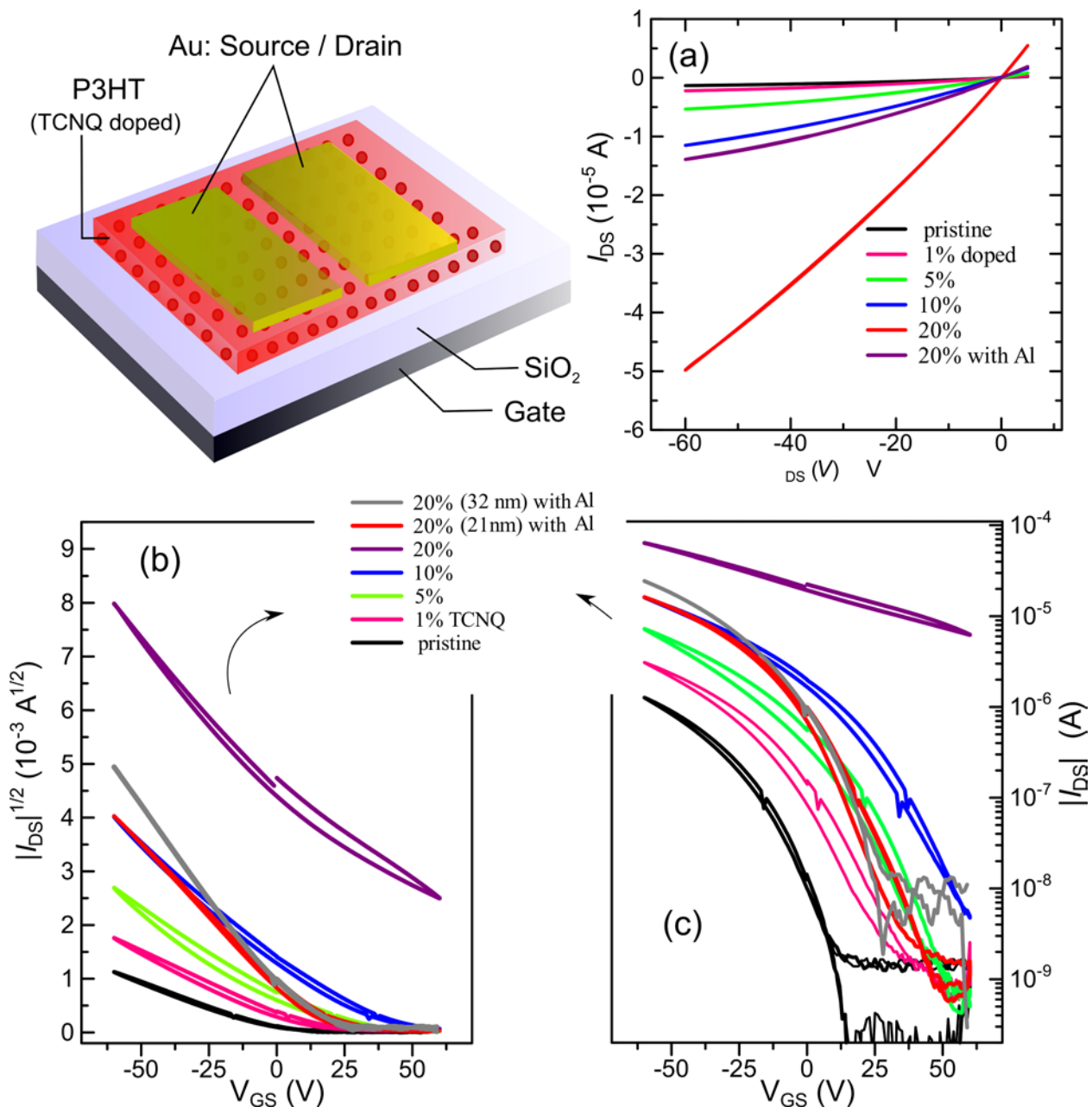


Figure 3

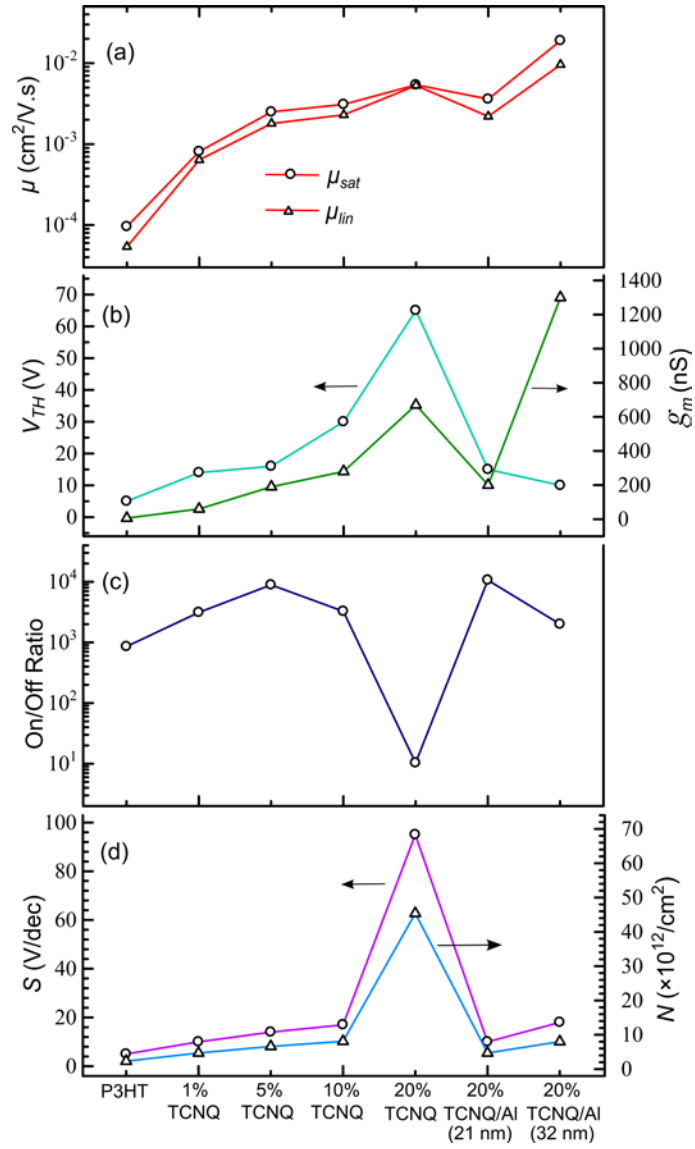


Figure 4

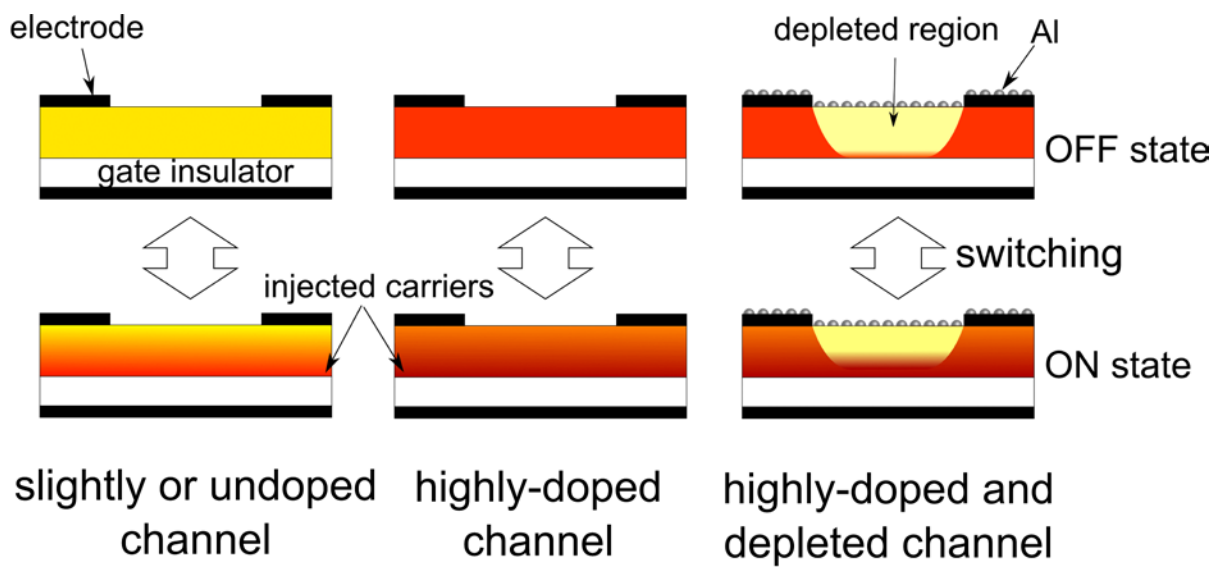


Figure 5